Effect of buoyancy-driven convection on steady state dendritic growth in a binary alloy*

Chen Ming-Wen (陈明文)[a)†], Wang Bao(王 宝)[a)], and Wang Zi-Dong(王自东)[b)‡]

[a)] School of Mathematics and Physics, University of Science and Technology Beijing, Beijing 100083, China
[b)] School of Materials Science and Engineering, University of Science and Technology Beijing, Beijing 100083, China

(Received 3 February 2013; revised manuscript received 12 June 2013)

The effect of buoyancy-driven convection on the steady state dendritic growth in an undercooled binary alloy is studied. For the case of the moderate modified Grashof number, the uniformly valid asymptotic solution in the entire region of space is obtained by means of the matched asymptotic expansion method. The analytical results show that the buoyancy-driven convection has a significant effect on the needle-like interface of dendritic growth. Due to the buoyancy-driven convection, the needle-like interface shape of the crystal is changed. When the Peclet number that is not affected by the buoyant flow is less than a certain critical value, the interface shape of the dendrite becomes thinner as the Grashof number increases; when it is larger than the critical value, the interface shape becomes fatter as the Grashof number increases. In the undercooled binary alloy the morphology number plays an active role in the interface shape and leads to the buoyancy effect that is different from the situation for the pure melt. The smaller the morphology number is, the more significant change the interface shape has. As the Peclet number further increases, the effect of buoyancy on the interface diminishes eventually.

Keywords: dendrite growth, convection, interface morphology, microgravity conditions

PACS: 68.70.+w, 81.10.Mx **DOI:** 10.1088/1674-1056/22/11/116805

1. Introduction

The effect of convective flow on dendritic growth under microgravity has been investigated during the past decades.[1–18] Huang and Glicksman[1] first carried out the important experimental investigation in the micro-gravity environment and found that buoyancy-driven convention has a profound effect on the growth speeds and the tip radii of the isolated dendrites. Rubinstein and Glicksman[3] found that dendrite growth velocity is an indication of the effect of interfacial energy anisotropy and buoyancy-driven convection. Baumgartl *et al.*[7] theoretically and experimentally studied the effect of buoyancy-driven convection and obtained a good correlation between the results of three-dimensional time-dependent numerical modeling, experimental modeling, and crystal growth of GaAs. Cai *et al.* [9] concluded that the combinative effect of buoyancy and surface tension convection enhances the homogeneity of the solute concentration and thus their morphological stability. Basil *et al.* [10] made numerical simulations as well as laboratory experiments of buoyancy-driven convection in an ampoule under varying heating and gravitational acceleration loadings and studied the nature and strength of the convective motion under low gravity conditions. Ananth *et al.*[11] and Schrage[12] performed theoretical analysis of a single dendrite for a simplified model of dendritic growth in the presence of natural convection and approximately solved the equations for the non-dimensional supercooling. Huo *et al.*, Zhu *et al.*[13–15] numerically studied the crystal growth under microgravity and concluded that there is possibly a stable growth interface with the upper end of the face tilting backwards. Huo *et al.*[16] found that there is possibly a stable growth face of the crystal under microgravity. Ge *et al.* [17] analyzed the influence of microgravity on the GaSb crystal and its potential developments in the future. Analytically, Canright and Davis[19] obtained a local solution valid near the interface for the steady state dendritic growth in an undercooled pure melt for the case of a small Grashof number, and concluded that when the Prandtl number and Stefan number are large enough, buoyancy enhances growth and distorts of the dendrite, whereas when the Prandtl number and Stefan number are small enough, buoyancy slows growth and flattens the tip. For the dendritic growth in the pure melt with buoyancy-driven convection, by using the matched asymptotic expansion method, Xu[20,21] obtained the uniformly valid asymptotic expansion for the steady state solution and revealed the stability mechanism of dendritic growth as well as the selection condition for the tip growth velocity.

The solute in the alloy melt alternates the interfacial temperature due to the Gibbs–Thomson condition and the solute segregation, hence, the effect of buoyancy-driven convection

*Project supported by the National Natural Science Foundation of China (Grant No. 10972030), the Fundamental Research Funds for the Central Universities of Ministry of Education of China (Grant No. FRF-BR-11-034B), and the Overseas Distinguished Scholar Program of the Ministry of Education of China (Grant No. MS2010bjkj005).

†Corresponding author. E-mail: chenmw@ustb.edu.cn
‡Corresponding author. E-mail: wangzd@mater.ustb.edu.cn

© 2013 Chinese Physical Society and IOP Publishing Ltd

on the dendritic growth from the binary alloy will be different from that on the dendritic growth from the pure melt. This paper aims to extend Xu's result in the pure melt to the case in the binary alloy. By using the matched asymptotic expansion method[20,22], we find the uniformly valid asymptotic solution for the steady state dendritic growth for the case of the moderate modified Grashof number and explore the growth mechanism of the dendritic growth in the binary alloy melt.

2. Mathematical model

Consider a single axi-symmetric dendrite growing in an undercooled binary alloy influenced by buoyancy-driven convection. Assume that the melt is the isotropy and incompressible Newtonian fluid, (Fig. 1), $(T_\infty)_{\rm D}$ and $(C_\infty)_{\rm D}$ are the dimensional temperature and concentration far from the dendrite, respectively, $\boldsymbol{g}$ is the gravitational acceleration along z positive direction downward into the undercooled melt, $(x,y,z)_{\rm D}$ denotes the dimensional rectangular coordinates, $(t)_{\rm D}$ denotes the dimensional time. The subscripts "D" refer to the dimensional quantities, respectively. We use the tip velocity V as the velocity scale, the diffusion length $\ell_{\rm D}=\kappa_{\rm D}/V$ as the length scale, where $\kappa_{\rm D}$ is the solute diffusivity in the liquid phase, $\Delta H/(c_{\rm p}\rho_{\rm L})$ as the temperature scale, where ΔH is the latent heat per unit volume of the solid, $c_{\rm p}$ is the specific heat, $\rho_{\rm L}$ is the density of the melt, and $(C_\infty)_{\rm D}$ as the concentration scale. Then, we introduce the following dimensionless variables (x,y,z), t, and physical quantities $\boldsymbol{U}$, $T_{\rm L}$, $T_{\rm S}$, $C_{\rm L}$, $C_{\rm S}$. The subscripts "S" and "L" refer to the solid phase and liquid phase, respectively. In the moving paraboloidal coordinate system (ξ,η,θ) that is fixed at the dendrite tip

$$r=\eta_0^2\xi\eta,\quad z=\frac{1}{2}\eta_0^2(\xi^2-\eta^2), \tag{1}$$

where the normalization parameter η_0^2 is to be determined by setting the location of the dendrite-tip, $r=\sqrt{x^2+y^2}$. The interface shape is expressed as $\eta=\eta_{\rm S}(\xi,\theta,t)$. In the paraboloidal coordinate system, the velocity field is written as $\boldsymbol{U}=\boldsymbol{U}(\xi,\eta,\theta,t)=(u,v,w)$. For the axi-symmetric dendrite, there is no flow in the azimuthal direction, θ, then the third component $w=0$, the vorticity vector $\boldsymbol{\Omega}=\boldsymbol{\nabla}\times\boldsymbol{U}=(0,0,\omega_3)$ has only one nonzero component, and the steady interface shape function is written as $\eta=\eta_{\rm S}(\xi,t)$. We choose the normalization parameter η_0^2 such that the steady interface shape satisfies the normalization condition

$$\eta_{\rm S}(0,t)=1, \tag{2}$$

and introduce the stream function $\psi=\psi(\xi,\eta,t)$ and vorticity function $\zeta(\xi,\eta,t)=\eta_0^2\xi\eta\omega_3$ such that

$$u=\frac{1}{\eta_0^4\xi\eta\sqrt{\xi^2+\eta^2}}\frac{\partial\psi}{\partial\eta},\quad v=\frac{-1}{\eta_0^4\xi\eta\sqrt{\xi^2+\eta^2}}\frac{\partial\psi}{\partial\xi}, \tag{3}$$

then the non-dimensional governing equations are expressed as follows.

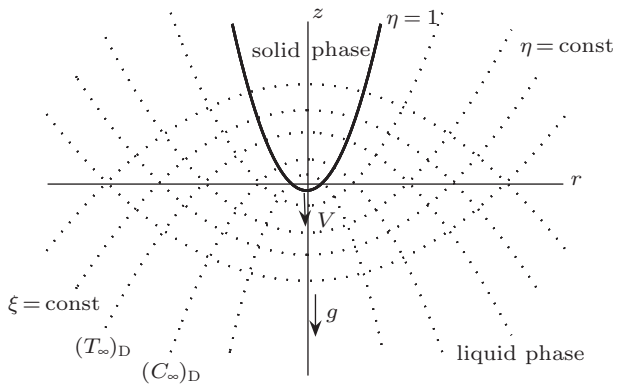


Fig. 1. The geometry of dendritic growth in an undercooled binary alloy with buoyancy-driven convection.

The kinematical equation

$$D^2\psi=-\eta_0^4(\xi^2+\eta^2)\zeta. \tag{4}$$

The vorticity equation

$$\begin{aligned}S_{\rm C}D^2\zeta\ =\ &\eta_0^4(\xi^2+\eta^2)\frac{\partial\zeta}{\partial t}\\&+\frac{2\zeta}{\eta_0^4\xi^2\eta^2}\frac{\partial(\psi,\eta_0^2\xi\eta)}{\partial(\xi,\eta)}-\frac{1}{\eta_0^2\xi\eta}\frac{\partial(\psi,\zeta)}{\partial(\xi,\eta)}\\&+\frac{\eta_0^4 Gr}{S_{\rm C}|T_\infty|}\xi\eta\left(\eta\frac{\partial T_{\rm L}}{\partial\xi}+\xi\frac{\partial T_{\rm L}}{\partial\eta}\right).\end{aligned} \tag{5}$$

The temperature equations in the liquid phase and solid phase

$$\boldsymbol{\nabla}^2T_{\rm L}=\lambda\eta_0^4(\xi^2+\eta^2)\frac{\partial T_{\rm L}}{\partial t}+\frac{\lambda}{\eta_0^2\xi\eta}\frac{\partial(T_{\rm L},\psi)}{\partial(\xi,\eta)}, \tag{6}$$

$$\boldsymbol{\nabla}^2T_{\rm S}=\lambda\alpha_{\rm T}\eta_0^4(\xi^2+\eta^2)\frac{\partial T_{\rm S}}{\partial t}+\lambda\alpha_{\rm T}(\xi\frac{\partial T_{\rm S}}{\partial\xi}-\eta\frac{\partial T_{\rm S}}{\partial\eta}). \tag{7}$$

The concentration equation in the liquid phase

$$\boldsymbol{\nabla}^2C_{\rm L}=\eta_0^4(\xi^2+\eta^2)\frac{\partial C_{\rm L}}{\partial t}+\frac{1}{\eta_0^2\xi\eta}\frac{\partial(C_{\rm L},\psi)}{\partial(\xi,\eta)}, \tag{8}$$

$$\boldsymbol{\nabla}^2C_{\rm S}=\alpha_{\rm C}\eta_0^4(\xi^2+\eta^2)\frac{\partial C_{\rm S}}{\partial t}+\alpha_{\rm C}(\xi\frac{\partial C_{\rm S}}{\partial\xi}-\eta\frac{\partial C_{\rm S}}{\partial\eta}), \tag{9}$$

where the operators $\boldsymbol{\nabla}^2$ and D^2 are defined as

$$\boldsymbol{\nabla}^2=\frac{\partial^2}{\partial\xi^2}+\frac{\partial^2}{\partial\eta^2}+\frac{1}{\xi}\frac{\partial}{\partial\xi}+\frac{1}{\eta}\frac{\partial}{\partial\eta},$$

$$D^2=\frac{\partial^2}{\partial\xi^2}+\frac{\partial^2}{\partial\eta^2}-\frac{1}{\xi}\frac{\partial}{\partial\xi}-\frac{1}{\eta}\frac{\partial}{\partial\eta},$$

and $\lambda=\kappa_{\rm D}/\kappa_{\rm T}$, $\alpha_{\rm T}=\kappa_{\rm T}/\kappa_{\rm S}$, $\alpha_{\rm C}=\kappa_{\rm D}/\kappa_{\rm SD}$, $\kappa_{\rm T}$ and $\kappa_{\rm S}$ are the thermal diffusivities in the liquid and solid phase, respectively, $\kappa_{\rm SD}$ is the solute diffusivity in the solid phase, $S_{\rm C}$ is the Schmidt number, $S_{\rm C}=\nu/\kappa_{\rm D}$, ν is the kinematical viscosity, and Gr is the Grashof number,

$$Gr=\frac{\beta g\kappa_{\rm T}}{\upsilon^3}\left((T_{\rm M})_{\rm D}-(T_\infty)_{\rm D}\right).$$

The non-dimensional boundary conditions are expressed as

$$\psi \sim \frac{1}{2}\eta_0^4\xi^2\eta^2 + o(1), \quad \zeta \to 0,$$
$$T_{\rm L} \to T_\infty, \quad C_{\rm L} \to 1 \ \text{ as } \ \eta \to \infty; \tag{10}$$
$$T_{\rm S} = O(1), \quad C_{\rm S} = O(1) \ \text{ as } \ \eta \to 0; \tag{11}$$
$$\psi = \zeta = \frac{\partial\psi}{\partial\xi} = \frac{\partial\zeta}{\partial\xi} = \frac{\partial\psi}{\partial\eta} = \frac{\partial\zeta}{\partial\eta} = \frac{\partial T_{\rm L}}{\partial\xi} = \frac{\partial C_{\rm L}}{\partial\xi} = 0$$
$$\text{as} \quad \xi = 0, \ \ \eta > 1, \tag{12}$$

and the interface conditions are as follows.

(i) the mass conservation condition

$$\frac{\partial\psi}{\partial\xi} + (\eta_{\rm S})'\frac{\partial\psi}{\partial\eta} = \eta_0^4\xi\eta_{\rm S}(\xi\eta_{\rm S})', \tag{13}$$

(ii) the continuity condition of the tangential component of velocity

$$-(\eta_{\rm S})'\frac{\partial\psi}{\partial\xi} + \frac{\partial\psi}{\partial\eta} + \eta_0^4\xi\eta_{\rm S}\left[\eta_{\rm S}(\eta_{\rm S})' - \xi\right] = 0, \tag{14}$$

(iii) the thermal dynamical equilibrium condition

$$T_{\rm L} = T_{\rm S}, \tag{15}$$

(iv) the Gibbs–Thomson condition

$$T_{\rm S} = -M_{\rm C}C_{\rm L}, \tag{16}$$

(v) the enthalpy conservation condition

$$\frac{1}{\lambda}\left[\frac{\partial T_{\rm L}}{\partial\eta} - (\eta_{\rm S})'\frac{\partial T_{\rm L}}{\partial\xi}\right] + \eta_0^2(\xi\eta_{\rm S})' = 0, \tag{17}$$

(vi) the mass conservation for the concentration

$$(C_{\rm L} - C_{\rm S})\eta_0^2(\xi\eta_{\rm S})' = -\left[\frac{\partial C_{\rm L}}{\partial\eta} - (\eta_{\rm S})'\frac{\partial C_{\rm L}}{\partial\xi}\right], \tag{18}$$

(vi) the concentration jump at the interface

$$C_{\rm S} = kC_{\rm L}, \tag{19}$$

where the notation prime represents the derivative with respect to ξ, $M_{\rm C}$ is the morphology number, $M_{\rm C} = -m(C_\infty)_{\rm D}/\left[\Delta H/(c_{\rm p}\rho_{\rm L})\right]$, with m being the liquidus slope, k is the segregation coefficient, $0 < k < 1$. In the present paper, the temperature and concentration in the solid phase are taken as constants, the densities in the liquid phase and solid phase are taken as equal, $\rho_{\rm L} = \rho_{\rm S}$, and surface tension and interface kinetics are negligible.

In order to use the Lagurre function for analysis, we use the transformation

$$\bar\sigma = \frac{\eta_0^2}{2S_{\rm C}}\xi^2, \quad \bar\tau = \frac{\eta_0^2}{2S_{\rm C}}\eta^2, \tag{20}$$
$$\psi = \psi_\infty + \bar\psi, \quad \zeta = \frac{1}{S_{\rm C}^2}\bar\zeta,$$
$$(\psi_\infty = \frac{1}{2}\eta_0^4\xi^2\eta^2 = 2S_{\rm C}^2\bar\sigma\bar\tau), \tag{21}$$
$$T_{\rm L} = T_\infty + S_{\rm C}\bar T_{\rm L}, \quad C_{\rm L} = 1 + S_{\rm C}\bar C_{\rm L}, \tag{22}$$

then the governing Eqs. (4)–(9) become

$$\bar\sigma\frac{\partial^2\bar\psi}{\partial\bar\sigma^2} + \bar\tau\frac{\partial^2\bar\psi}{\partial\bar\tau^2} = -(\bar\sigma + \bar\tau)\bar\zeta, \tag{23}$$
$$\bar\sigma\frac{\partial^2\bar\zeta}{\partial\bar\sigma^2} + \bar\tau\frac{\partial^2\bar\zeta}{\partial\bar\tau^2}$$
$$= \bar\sigma\frac{\partial\bar\zeta}{\partial\bar\sigma} - \bar\tau\frac{\partial\bar\zeta}{\partial\bar\tau} + \frac{1}{2S_{\rm C}^2}\frac{\bar\zeta}{\bar\sigma\bar\tau}\left(\bar\sigma\frac{\partial\bar\psi}{\partial\bar\sigma} - \bar\tau\frac{\partial\bar\psi}{\partial\bar\tau}\right)$$
$$-\frac{1}{2S_{\rm C}^2}\frac{\partial(\bar\psi,\bar\zeta)}{\partial(\bar\sigma,\bar\tau)} + \bar G\bar\sigma\bar\tau\left(\frac{\partial\bar T_{\rm L}}{\partial\bar\sigma} + \frac{\partial\bar T_{\rm L}}{\partial\bar\tau}\right), \tag{24}$$
$$\bar\sigma\frac{\partial^2\bar T_{\rm L}}{\partial\bar\sigma^2} + \bar\tau\frac{\partial^2\bar T_{\rm L}}{\partial\bar\tau^2} + \frac{\partial\bar T_{\rm L}}{\partial\bar\sigma} + \frac{\partial\bar T_{\rm L}}{\partial\bar\tau}$$
$$= \lambda S_{\rm C}\left(\bar\sigma\frac{\partial\bar T_{\rm L}}{\partial\bar\sigma} - \bar\tau\frac{\partial\bar T_{\rm L}}{\partial\bar\tau}\right) + \frac{\lambda}{2S_{\rm C}}\frac{\partial(\bar T_{\rm L},\bar\psi)}{\partial(\bar\sigma,\bar\tau)}, \tag{25}$$
$$\bar\sigma\frac{\partial^2\bar C_{\rm L}}{\partial\bar\sigma^2} + \bar\tau\frac{\partial^2\bar C_{\rm L}}{\partial\bar\tau^2} + \frac{\partial\bar C_{\rm L}}{\partial\bar\sigma} + \frac{\partial\bar C_{\rm L}}{\partial\bar\tau}$$
$$= S_{\rm C}\left(\bar\sigma\frac{\partial\bar C_{\rm L}}{\partial\bar\sigma} - \bar\tau\frac{\partial\bar C_{\rm L}}{\partial\bar\tau}\right) + \frac{1}{2S_{\rm C}}\frac{\partial(\bar C_{\rm L},\bar\psi)}{\partial(\bar\sigma,\bar\tau)}, \tag{26}$$

where $\bar G$ represents the modified Grashof number

$$\bar G = \frac{2S_{\rm C}^3 Gr}{|T_\infty|}. \tag{27}$$

The interface conditions (13)–(19) at the interface $\bar\tau = \bar\tau_{\rm S}(\bar\sigma,\varepsilon)$ become

$$\frac{\partial\bar\psi}{\partial\bar\sigma} + (\bar\tau_{\rm S})'\frac{\partial\bar\psi}{\partial\bar\tau} = 0, \tag{28}$$
$$\bar\tau_{\rm S}\frac{\partial\bar\psi}{\partial\bar\tau} - \bar\sigma(\bar\tau_{\rm S})'\frac{\partial\bar\psi}{\partial\bar\sigma} = 0, \tag{29}$$
$$S_{\rm C}(\bar T_{\rm L} + M_{\rm C}\bar C_{\rm L}) = -(T_\infty + M_{\rm C}), \tag{30}$$
$$\frac{1}{\lambda}\left[\bar\tau_{\rm S}\frac{\partial\bar T_{\rm L}}{\partial\bar\tau} - \bar\sigma(\bar\tau_{\rm S})'\frac{\partial\bar T_{\rm L}}{\partial\bar\sigma}\right] + \bar\tau_{\rm S} + \bar\sigma(\bar\tau_{\rm S})' = 0, \tag{31}$$
$$S_{\rm C}(1-k)[\bar\tau_{\rm S} + \bar\sigma(\bar\tau_{\rm S})']\bar C_{\rm L} + (1-k)[\bar\tau_{\rm S} + \bar\sigma(\bar\tau_{\rm S})']$$
$$+\left[\bar\tau_{\rm S}\frac{\partial\bar C_{\rm L}}{\partial\bar\tau} - \bar\sigma(\bar\tau_{\rm S})'\frac{\partial\bar C_{\rm L}}{\partial\bar\sigma}\right] = 0, \tag{32}$$

where the notation prime represents the derivative with respect to $\bar\sigma$.

For typical metals, the Schmidt number is large and we adopt its reciprocal number as a small parameter

$$\varepsilon = \frac{1}{S_{\rm C}}, \tag{33}$$

then the interface shape function is written as the form

$$\bar\tau = \bar\tau_{\rm S}(\bar\sigma,\varepsilon) = \varepsilon\frac{\eta_0^2}{2}\eta_{\rm S}^2 = O(\varepsilon). \tag{34}$$

The normalization condition of the interface shape $\eta_{\rm S}(0,t) = 1$ is rewritten as

$$\bar\tau_{\rm S}(0,\varepsilon) = \bar\tau_0 = \varepsilon\frac{\eta_0^2}{2}. \tag{35}$$

For the small parameter ε, the above solidification system under study constitutes a singular boundary problem. We seek a uniformly valid asymptotic expansion solution for the steady state of the binary alloy as $\varepsilon \to 0$.

3. Asymptotic expansion solution in the Laguerre series

Since the viscous effect is dominant near the interface while the inertia effect is dominant in the region far from the interface, the interaction between convection and the interface morphology behaves differently in different parts of the melt region. Similar to the treatment made by Xu,[20,21] we divide the whole region into two sub-regions: the inner region near the interface $\bar{\tau} \ll 1$; the outer region away from the interface $\bar{\tau} = O(1)$. We seek the outer expansion solution and inner expansion solution in each sub-region, respectively, and match them to obtain a uniformly valid asymptotic solution. Due to the effect of the flow field on the temperature and concentration fields, we first find the inner solution for the binary alloy, then solve the outer solution for the temperature and concentration fields.

In the inner region, we use the inner variable $(\bar{\sigma}, \hat{\tau})$

$$\hat{\tau} = \frac{\bar{\tau}}{\varepsilon}, \tag{36}$$

then $\bar{\tau}_0 = \varepsilon\hat{\tau}_0$, $\hat{\tau}_0 = \eta_0^2/2 = O(1)$, and write for the flow field

$$\psi = \psi^*(\bar{\sigma}, \hat{\tau}) + \hat{\psi}(\bar{\sigma}, \hat{\tau}, \varepsilon), \quad \varsigma = \varepsilon^2\hat{\varsigma}(\bar{\sigma}, \hat{\tau}, \varepsilon), \tag{37}$$

where $\psi^* = 2\bar{\sigma}\hat{\tau}/\varepsilon$, $\hat{\varsigma}(\bar{\sigma}, \hat{\tau}, \varepsilon) = \bar{\varsigma}(\bar{\sigma}, \varepsilon\hat{\tau}, \varepsilon)$, $\hat{\psi}(\bar{\sigma}, \hat{\tau}, \varepsilon) = \bar{\psi}(\bar{\sigma}, \varepsilon\hat{\tau}, \varepsilon)$, the inner solution $\hat{\varsigma}$ and $\hat{\psi}$ have the asymptotic expansions

$$\begin{aligned}\hat{\psi} &= \varepsilon\hat{\upsilon}_0(\varepsilon)\hat{\psi}_0(\bar{\sigma}, \hat{\tau}) + \varepsilon\hat{\upsilon}_1(\varepsilon)\hat{\psi}_1(\bar{\sigma}, \hat{\tau}) \\ &\quad + \varepsilon\hat{\upsilon}_2(\varepsilon)\hat{\psi}_2(\bar{\sigma}, \hat{\tau}) + \cdots, \end{aligned} \tag{38}$$

$$\begin{aligned}\hat{\varsigma} &= \varepsilon\hat{\upsilon}_0(\varepsilon)\hat{\varsigma}_0(\bar{\sigma}, \hat{\tau}) + \varepsilon\hat{\upsilon}_1(\varepsilon)\hat{\varsigma}_1(\bar{\sigma}, \hat{\tau}) \\ &\quad + \varepsilon\hat{\upsilon}_2(\varepsilon)\hat{\varsigma}_2(\bar{\sigma}, \hat{\tau}) + \cdots, \end{aligned} \tag{39}$$

where asymptotic sequence $\hat{\upsilon}_n(\varepsilon)$ are to be determined, and $\hat{\psi}_n$ and $\hat{\varsigma}_n$ have the Laguerre series expansions

$$\begin{aligned}\hat{\psi}_n &= \hat{B}_{n,0}(\hat{\tau})\bar{\sigma}L_0^{(1)}(\bar{\sigma}) + \hat{B}_{n,1}(\hat{\tau})\bar{\sigma}L_1^{(1)}(\bar{\sigma}) \\ &\quad + \hat{B}_{n,2}(\hat{\tau})\bar{\sigma}L_2^{(1)}(\bar{\sigma}) + \cdots, \end{aligned} \tag{40}$$

$$\begin{aligned}\hat{\varsigma}_n &= \hat{A}_{n,0}(\hat{\tau})\bar{\sigma}L_0^{(1)}(\bar{\sigma}) + \hat{A}_{n,1}(\hat{\tau})\bar{\sigma}L_1^{(1)}(\bar{\sigma}) \\ &\quad + \hat{A}_{n,2}(\hat{\tau})\bar{\sigma}L_2^{(1)}(\bar{\sigma}) + \cdots. \end{aligned} \tag{41}$$

With the result made by Xu,[18,19] taking $\hat{\nu}_0(\varepsilon) = \varepsilon^2$, we derive that

$$\hat{A}_{0,0} = \bar{G}I_{0,0}\left(\lambda\hat{\tau}E_1(\lambda\hat{\tau}) - e^{-\lambda\hat{\tau}}\right),$$

$$\hat{B}_{0,0} = -\frac{2}{\lambda}\bar{G}I_{0,0}\left[Q_0(\lambda\hat{\tau}) - Q_0(\lambda\hat{\tau}) - \lambda Q_0'(\lambda\hat{\tau}_{0,0})(\hat{\tau} - \hat{\tau}_{0,0})\right],$$

$$\hat{B}_{1,0} = -\frac{1}{2}\hat{B}_{0,0},$$

$$\hat{A}_{n,0} = 0 \quad (n = 1,2,3,\cdots), \quad \hat{B}_{n,0} = 0 \quad (n = 2,3,4,\cdots),$$

where

$$Q_0(s) = \frac{1}{2}s(2+s)E_1(s) - \frac{1}{2}(1+s)\,\mathrm{e}^{-s}.$$

We obtain the inner solution of the flow field

$$\begin{aligned}\hat{\psi} &= -\frac{\varepsilon^2}{\lambda}\bar{G}I_{0,0}\bar{\sigma}\left[Q_0(\lambda\hat{\tau}) - Q_0(\lambda\hat{\tau}) - \lambda Q_0'(\lambda\hat{\tau}_{0,0})(\hat{\tau} - \hat{\tau}_{0,0})\right] \\ &\quad \times \left[2L_0^{(1)}(\bar{\sigma}) - L_1^{(1)}(\bar{\sigma})\right] + O(\varepsilon^4), \end{aligned} \tag{42}$$

$$\hat{\varsigma} = \varepsilon\bar{G}I_{0,0}\left[\lambda\hat{\tau}E_1(\lambda\hat{\tau}) - e^{-\lambda\hat{\tau}}\right]\bar{\sigma} + O(\varepsilon^2)). \tag{43}$$

With the inner variable $(\bar{\sigma}, \hat{\tau})$, we rewrite the interface function

$$\hat{\tau} = \hat{\tau}_{\mathrm{S}}(\bar{\sigma}, \varepsilon) = \hat{\tau}_0(\varepsilon) + \hat{h}_{\mathrm{S}}(\bar{\sigma}, \varepsilon), \tag{44}$$

where $\hat{h}_{\mathrm{S}}(0, \varepsilon) = 0$, $|\hat{h}_{\mathrm{S}}| \ll \hat{\tau}_0$, and expand $\hat{\tau}_0(\varepsilon)$ and $\hat{h}_{\mathrm{S}}(\bar{\sigma}, \varepsilon)$ in the asymptotic series

$$\hat{\tau}_0(\varepsilon) = \hat{\tau}_{0,0} + \tilde{\tau}_0(\varepsilon) = \hat{\tau}_{0,0} + \hat{\delta}_0(\varepsilon)\hat{\tau}_{1,0} + \hat{\delta}_1(\varepsilon)\hat{\tau}_{2,0} + \cdots, \tag{45}$$

$$\hat{h}_{\mathrm{S}} = \hat{\delta}_0(\varepsilon)\hat{h}_0 + \hat{\delta}_1(\varepsilon)\hat{h}_1 + \hat{\delta}_2(\varepsilon)\hat{h}_2 + \cdots, \tag{46}$$

where asymptotic sequence $\hat{\delta}_n(\varepsilon)$ are to be determined and $\hat{h}_n$ have the Laguerre series expansions

$$\hat{h}_n = \hat{h}_{n,0}L_0^{(1)}(\bar{\sigma}) + \hat{h}_{n,1}L_1^{(1)}(\bar{\sigma}) + \cdots. \tag{47}$$

From $\hat{h}_{\mathrm{S}}(0, \varepsilon) = 0$, it yields that $\bar{\tau}_{\mathrm{S}}(0) = \bar{\tau}_0 = \varepsilon\eta_0^2/2$, then

$$\hat{h}_n(0) = 0, \quad n = 0,1,2,\ldots. \tag{48}$$

For the temperature field and concentration field, we have the asymptotic expansions

$$\begin{aligned}T_{\mathrm{L}} - T_\infty &= S_{\mathrm{C}}\hat{T}_{\mathrm{L}}(\bar{\sigma}, \hat{\tau}, \varepsilon) \\ &= S_{\mathrm{C}}\left[\hat{\delta}_0(\varepsilon)\hat{T}_0(\bar{\sigma}, \hat{\tau}) + \hat{\delta}_1(\varepsilon)\hat{T}_1(\bar{\sigma}, \hat{\tau}) + \cdots\right], \end{aligned} \tag{49}$$

$$\begin{aligned}C_{\mathrm{L}} - 1 &= S_{\mathrm{C}}\hat{C}(\bar{\sigma}, \hat{\tau}, \varepsilon) \\ &= S_{\mathrm{C}}\left[\hat{\delta}_0(\varepsilon)\hat{C}_0(\bar{\sigma}, \hat{\tau}) + \hat{\delta}_1(\varepsilon)\hat{C}_1(\bar{\sigma}, \hat{\tau}) + \cdots\right], \end{aligned} \tag{50}$$

in which, $\hat{T}_n$ and $\hat{C}_n$ have the Laguerre series expansions

$$\hat{T}_n = \hat{D}_{n,0}(\hat{\tau})L_0^{(1)}(\bar{\sigma}) + \hat{D}_{n,1}(\hat{\tau})L_1^{(1)}(\bar{\sigma}) + \cdots, \tag{51}$$

$$\hat{C}_n = \hat{E}_{n,0}(\hat{\tau})L_0^{(1)}(\bar{\sigma}) + \hat{E}_{n,1}(\hat{\tau})L_1^{(1)}(\bar{\sigma}) + \cdots. \tag{52}$$

For the leading order term in Eqs. (49)–(50), we can take $\delta_0(\varepsilon) = \varepsilon$, similar to the Xu's treatment,[19,20] we have

$$\hat{D}_{n,0} = 0, \quad \hat{E}_{n,0} = 0, \quad n = 1,2,\ldots, \tag{53}$$

$$\hat{D}_{0,0} = \lambda I_{0,0}E_1(\lambda\hat{\tau}), \quad \hat{E}_{0,0} = I_{0,0}^{\mathrm{C}}E_1(\hat{\tau}), \tag{54}$$

$$T_\infty = -\lambda\hat{\tau}_{0,0}\mathrm{e}^{\lambda\hat{\tau}_{0,0}}E_1(\lambda\hat{\tau}_{0,0}) - M_{\mathrm{C}} - M_{\mathrm{C}}I_{0,0}^{\mathrm{C}}\mathrm{e}^{\hat{\tau}_{0,0}}E_1(\hat{\tau}_{0,0}), \tag{55}$$

where $E_1(x)$ is the exponential function

$$E_1(x) = \int_x^{+\infty}\frac{\mathrm{e}^{-t}}{t}\,\mathrm{d}t, \quad I_{0,0} = \hat{\tau}_{0,0}\mathrm{e}^{\lambda\hat{\tau}_{0,0}},$$

$$I^{\mathrm{C}}_{0,0} = \frac{\hat{\tau}_{0,0}(1-k)\,\mathrm{e}^{\hat{\tau}_{0,0}}}{1-(1-k)\,\hat{\tau}_{0,0}E_1(\hat{\tau}_{0,0})\,\mathrm{e}^{\hat{\tau}_{0,0}}}.$$

This formula is the generalization of the famous Ivantsov solution.[20,23] If $M_{\mathrm{C}} = 0$, equation (55) reduces to the Ivantsov solution,

$$T_\infty = -\frac{\lambda\eta^2_{0,0}}{2}\mathrm{e}^{\lambda\eta^2_{0,0}/2}E_1\left(\frac{\lambda\eta^2_{0,0}}{2}\right),$$

or

$$T_\infty = -\lambda\,\hat{\tau}_{0,0}\mathrm{e}^{\lambda\,\hat{\tau}_{0,0}}E_1(\lambda\,\hat{\tau}_{0,0}),$$

which is the same as that for the case of the pure melt obtained by Xu.[19,20] It can be seen that $\hat{\tau}_{0,0}$ depends on the undercooling parameter T_∞ and the morphology number M_{C}. In Figs. 2 and 3, we show, respectively, the solutions of the temperature $\hat{T}_0$ and concentration $\hat{C}_0$ for the cases: $\hat{\tau}_{0,0} = 0.20$, 0.50, 1.00, 1.50, $M_{\mathrm{C}} = 0.20$, $k = 0.30$, and $\lambda = 0.001$. In Fig. 4, we show the variations of undercooling temperature T_∞ with variable $\hat{\tau}_{0,0}$ in the binary alloy for different values: $M_{\mathrm{C}} = 0$, 0.10, 0.20, 0.30 and $k = 0.3$, $\lambda = 0.001$.

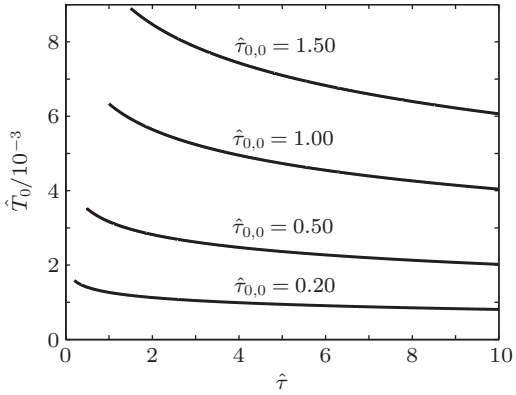


Fig. 2. The solutions of temperature $\hat{T}_0$ versus variable $\hat{\tau}$for the cases: $\hat{\tau}_{0,0} = 0.20$, 0.50, 1.00, 1.50 from bottom to top in the undercooled binary melt with $\lambda = 0.001$, $M_{\mathrm{C}} = 0.20$, $k = 0.3$.

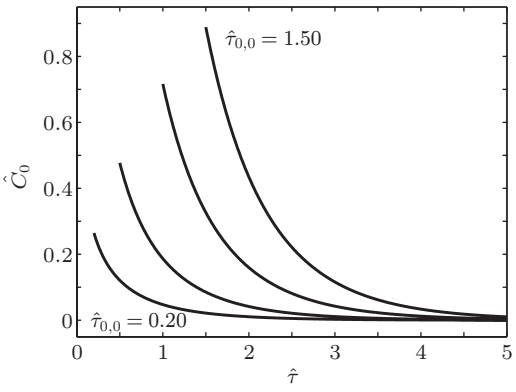


Fig. 3. The solutions of concentration $\hat{C}_0$ versus variable $\hat{\tau}$for the cases: $\hat{\tau}_{0,0} = 0.20$, 0.50, 1.00, 1.50 from bottom to top in the undercooled binary melt with $\lambda = 0.001$, $M_{\mathrm{C}} = 0.20$, $k = 0.3$.

From $\hat{h}_{\mathrm{S}}(0,\varepsilon) = 0$, we obtain that

$$\hat{h}_{0,0} = 0. \tag{56}$$

Due to the buoyancy effect, the non-uniform temperature distribution induces a perturbed flow field in the inner region.

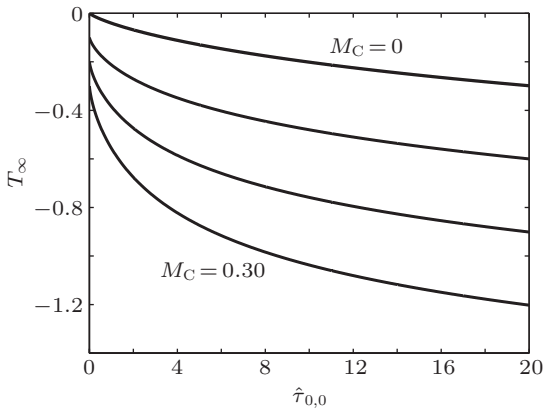


Fig. 4. The variations of undercooling temperature T_∞ with variable $\hat{\tau}_{0,0}$ in the binary alloy for different values: $M_{\mathrm{C}} = 0$, 0.10, 0.20, 0.30 (from top to bottom) in the undercooled binary melt with $k = 0.3$, $\lambda = 0.001$.

The above solution is divergent for any fixed $\bar{\sigma}$ when $\hat{\tau} \to \infty$, and then not uniformly valid in the far field. Thus we turn to seek the outer solution and match it with the inner solution.

In the outer region $\bar{\tau} = O(1)$, we seek the asymptotic expansion in Eqs. (36)–(40) as $\varepsilon \to 0$ for the flow field

$$\begin{aligned}\bar{\varsigma} &= \upsilon_0(\varepsilon)\varsigma_0(\bar{\sigma},\bar{\tau}) + \upsilon_1(\varepsilon)\varsigma_1(\bar{\sigma},\bar{\tau}) + \cdots \\ &\quad + \upsilon_n(\varepsilon)\varsigma_n(\bar{\sigma},\bar{\tau}) + \cdots, \qquad (57)\\ \bar{\psi} &= \upsilon_0(\varepsilon)\psi_0(\bar{\sigma},\bar{\tau}) + \upsilon_1(\varepsilon)\psi_1(\bar{\sigma},\bar{\tau}) + \cdots \\ &\quad + \upsilon_n(\varepsilon)\psi_n(\bar{\sigma},\bar{\tau}) + \cdots, \qquad (58)\end{aligned}$$

in which, asymptotic sequences $\upsilon_n(\varepsilon)$ are to be determined, and ς_n and ψ_n have Lagurrer series expansions

$$\varsigma_n = A_{n,0}(\bar{\tau})\bar{\sigma}L^{(1)}_0(\bar{\sigma}) + A_{n,1}(\bar{\tau})\bar{\sigma}L^{(1)}_0(\bar{\sigma}) + \cdots, \tag{59}$$

$$\psi_n = B_{n,0}(\bar{\tau})\bar{\sigma}L^{(1)}_0(\bar{\sigma}) + B_{n,1}(\bar{\tau})\bar{\sigma}L^{(1)}_0(\bar{\sigma}) + \cdots. \tag{60}$$

Similar to the result in the pure melt made by Xu[20,21], the outer solution of the stream function

$$\begin{aligned}\bar{\psi} &= \frac{\varepsilon^2}{\ln\varepsilon}\{b_{0,0}E_2(\hat{\tau})\bar{\sigma} - \psi^*_0(\bar{\sigma},\bar{\tau}) \\ &\quad + b_{0,1}\left[3E_4(\hat{\tau}) - 2E_3(\hat{\tau})\right]\bar{\sigma}L^{(1)}_1(\bar{\sigma}) \\ &\quad - \frac{1}{2}\psi^*_1(\bar{\sigma},\bar{\tau})\} + o\left(\frac{\varepsilon^2}{\ln\varepsilon}\right), \qquad (61)\\ \bar{\zeta} &= -\frac{\varepsilon^2}{\ln\varepsilon}\{b_{0,0}E_2(\hat{\tau})\bar{\sigma} - \psi^*_0(\bar{\sigma},\bar{\tau}) \\ &\quad + b_{0,1}\left[3E_4(\hat{\tau}) - 2E_3(\hat{\tau})\right]\bar{\sigma}L^{(1)}_1(\bar{\sigma}) \\ &\quad - \frac{1}{2}\psi^*_1(\bar{\sigma},\bar{\tau})\} + o\left(\frac{\varepsilon^2}{\ln\varepsilon}\right), \qquad (62)\end{aligned}$$

where $\bar{\psi}^*_0$ and $\bar{\psi}^*_1$ are two determined special outer solution,[20] and

$$b_{0,0} = \frac{2}{\lambda}\bar{G}I_{0,0}Q'_0(\lambda\,\hat{\tau}_{0,0}),$$

$$b_{0,1} = -\frac{1}{\lambda}\bar{G}I_{0,0}Q_0'(\lambda\hat{\tau}_{0,0}), \quad E_m(\bar{\tau}) = \int_1^\infty \frac{\mathrm{e}^{-\bar{\tau}t}}{t^m}\mathrm{d}t.$$

From Eqs. (A7) and (A8), it is seen that the second sequences $\hat{\delta}_1\hat{T}_1$ and $\hat{\delta}_1\hat{C}_1$ are only affected by the first sequence of flow field $\varepsilon^3\hat{v}_0(\varepsilon)\hat{\psi}_0$, which only involve the components $L_0^{(1)}(\bar{\sigma})$ and $L_1^{(1)}(\bar{\sigma})$, then

$$\hat{T}_1 = \hat{D}_{1,0}L_0^{(1)}(\bar{\sigma}) + \hat{D}_{1,1}L_1^{(1)}(\bar{\sigma}), \tag{63}$$

$$\hat{C}_1 = \hat{E}_{1,0}L_0^{(1)}(\bar{\sigma}) + \hat{E}_{1,1}L_1^{(1)}(\bar{\sigma}). \tag{64}$$

Due to $\varepsilon\hat{v}_0(\varepsilon)\hat{\psi}_0 = O(\varepsilon^3)$, the interaction terms in Eqs. (A1) and (A2) have the orders of magnitude

$$\frac{\varepsilon}{2}N_{\mathrm{T}}(\hat{T}_0, \hat{\psi}_0) = O(\varepsilon^4), \quad \frac{\varepsilon}{2}N_{\mathrm{T}}(\hat{C}_0, \hat{\psi}_0) = O(\varepsilon^4),$$

we take $\delta_1(\varepsilon) = \varepsilon^5$, then the governing equations for $\hat{D}_{1,0}$, $\hat{D}_{1,1}$, $\hat{E}_{1,0}$, and $\hat{E}_{1,1}$ are

$$\frac{\mathrm{d}^2\hat{D}_{1,0}}{\mathrm{d}\hat{\tau}^2} + \left(\lambda + \frac{1}{\hat{\tau}}\right)\frac{\mathrm{d}\hat{D}_{1,0}}{\mathrm{d}\hat{\tau}} = -2\lambda\bar{G}I_{0,0}^2\hat{H}_0(\hat{\tau},\lambda), \tag{65}$$

$$\frac{\mathrm{d}^2\hat{D}_{1,1}}{\mathrm{d}\hat{\tau}^2} + \left(\lambda + \frac{1}{\hat{\tau}}\right)\frac{\mathrm{d}\hat{D}_{1,1}}{\mathrm{d}\hat{\tau}} = \lambda\bar{G}I_{0,0}^2\hat{H}_0(\hat{\tau},\lambda), \tag{66}$$

$$\begin{aligned}&\hat{\tau}\frac{\mathrm{d}^2\hat{E}_{1,0}}{\mathrm{d}\hat{\tau}^2} + (\lambda\hat{\tau}+1)\frac{\mathrm{d}\hat{E}_{1,0}}{\mathrm{d}\hat{\tau}}\\ &= -\frac{2}{\lambda}\bar{G}I_{0,0}I_{0,0}^{\mathrm{C}}\hat{\tau}\mathrm{e}^{(\lambda-1)\hat{\tau}}\hat{H}_0(\hat{\tau},\lambda),\end{aligned} \tag{67}$$

$$\begin{aligned}&\hat{\tau}\frac{\mathrm{d}^2\hat{D}_{1,1}}{\mathrm{d}\hat{\tau}^2} + (\lambda\hat{\tau}+1)\frac{\mathrm{d}\hat{D}_{1,1}}{\mathrm{d}\hat{\tau}}\\ &= \frac{1}{\lambda}\bar{G}I_{0,0}I_{0,0}^{\mathrm{C}}\hat{\tau}\hat{H}_0(\hat{\tau},\lambda)\mathrm{e}^{(\lambda-1)\hat{\tau}},\end{aligned} \tag{68}$$

where

$$\begin{aligned}\hat{H}_0(\hat{\tau},\lambda) = {}& \frac{\mathrm{e}^{-\lambda\hat{\tau}}}{\hat{\tau}^2}[Q_0(\lambda\hat{\tau}) - Q_0(\lambda\hat{\tau}_{0,0})\\ &- \lambda Q_0'(\lambda\hat{\tau}_{0,0})(\hat{\tau} - \hat{\tau}_{0,0})].\end{aligned}$$

The interface conditions: at the interface $\hat{\tau} = \hat{\tau}_{0,0}$,

$$\hat{D}_{1,0} + M_{\mathrm{C}}\hat{E}_{1,0} + \left(\frac{\mathrm{d}\hat{D}_{0,0}}{\mathrm{d}\hat{\tau}} + M_{\mathrm{C}}\frac{\mathrm{d}\hat{E}_{0,0}}{\mathrm{d}\hat{\tau}}\right)\hat{\tau}_{1,0} = 0, \tag{69}$$

$$\frac{1}{\lambda}\hat{\tau}_{0,0}\frac{\mathrm{d}\hat{D}_{1,0}}{\mathrm{d}\hat{\tau}} + (1+\lambda\hat{\tau}_{0,0})\hat{\tau}_{1,0} - 2\hat{h}_{0,1} = 0, \tag{70}$$

$$\begin{aligned}&\hat{\tau}_{0,0}\frac{\mathrm{d}\hat{E}_{1,0}}{\mathrm{d}\hat{\tau}} + (1-k)\hat{\tau}_{0,0}\hat{E}_{1,0}\\ &+ (1-k)(1+k\hat{\tau}_{0,0})(1+\hat{E}_{0,0})\hat{\tau}_{1,0}\\ &= 2(1-k)(1+\hat{E}_{0,0})\hat{h}_{0,1},\end{aligned} \tag{71}$$

$$\hat{D}_{1,1} + M_{\mathrm{C}}\hat{E}_{1,1} + \left(\frac{\mathrm{d}\hat{D}_{0,0}}{\mathrm{d}\hat{\tau}} + M_{\mathrm{C}}\frac{\mathrm{d}\hat{E}_{0,0}}{\mathrm{d}\hat{\tau}}\right)\hat{h}_{0,1} = 0, \tag{72}$$

$$\frac{1}{\lambda}\hat{\tau}_{0,0}\frac{\mathrm{d}\hat{D}_{1,1}}{\mathrm{d}\hat{\tau}} + (1+\lambda\hat{\tau}_{0,0})\hat{\tau}_{1,0} + \hat{h}_{0,1} = 0, \tag{73}$$

$$\begin{aligned}&\hat{\tau}_{0,0}\frac{\mathrm{d}\hat{E}_{1,1}}{\mathrm{d}\hat{\tau}} + (1-k)\hat{\tau}_{0,0}\hat{E}_{1,1}\\ &+ (1-k)(2+k\hat{\tau}_{0,0})(1+\hat{E}_{0,0})\hat{h}_{0,1} = 0.\end{aligned} \tag{74}$$

The general solutions of Eqs. (65)–(68) with the vanishing conditions at the far field are of the forms

$$\hat{D}_{1,0}(\hat{\tau}) = I_{1,0}E_1(\lambda\hat{\tau}) - 2\lambda\bar{G}I_{0,0}^2\hat{R}_0(\hat{\tau}), \tag{75}$$

$$\hat{D}_{1,1}(\hat{\tau}) = I_{1,1}E_1(\lambda\hat{\tau}) + \lambda\bar{G}I_{0,0}^2\hat{R}_0(\hat{\tau}), \tag{76}$$

$$\hat{E}_{1,0}(\hat{\tau}) = I_{1,0}^{\mathrm{C}}E_1(\hat{\tau}) - \frac{2}{\lambda}\bar{G}I_{0,0}I_{0,0}^{\mathrm{C}}\hat{R}_1(\hat{\tau}), \tag{77}$$

$$\hat{E}_{1,1}(\hat{\tau}) = I_{1,1}^{\mathrm{C}}E_1(\hat{\tau}) + \frac{1}{\lambda}\bar{G}I_{0,0}I_{0,0}^{\mathrm{C}}\hat{R}_1(\hat{\tau}), \tag{78}$$

where $E_1(t)$ is the exponential integral, and

$$\begin{aligned}\hat{R}_0(\hat{\tau}) = {}& -\int_{\hat{\tau}}^{\infty}\frac{\mathrm{e}^{-\lambda x}}{x}\mathrm{d}x\int_{\hat{\tau}_{0,0}}^{x}[Q_0(\lambda y) - Q_0(\lambda\hat{\tau}_{0,0})\\ &- \lambda Q_0'(\lambda\hat{\tau}_{0,0})(y - \hat{\tau}_{0,0})]\frac{1}{y}\mathrm{d}y,\end{aligned} \tag{79}$$

$$\begin{aligned}\hat{R}_1(\hat{\tau}) = {}& -\int_{\hat{\tau}}^{\infty}\frac{\mathrm{e}^{-x}}{x}\mathrm{d}x\int_{\hat{\tau}_{0,0}}^{x}[Q_0(\lambda y) - Q_0(\lambda\hat{\tau}_{0,0})\\ &- \lambda Q_0'(\lambda\hat{\tau}_{0,0})(y - \hat{\tau}_{0,0})]\frac{1}{y}\mathrm{d}y.\end{aligned} \tag{80}$$

With the interface conditions (69)–(74), we have

$$I_{1,0} = 2\lambda\frac{[O_1O_2 - M_{\mathrm{C}}O_3 - (O_2+\lambda)(1+\lambda\hat{\tau}_{0,0})]\hat{h}_{0,1} + (1+\lambda\hat{\tau}_{0,0})(M_{\mathrm{C}}b_3 - O_1b_1)}{-O_1O_2\mathrm{e}^{-\lambda\hat{\tau}_{0,0}} - \lambda O_1(1+\lambda\hat{\tau}_{0,0}) + M_{\mathrm{C}}O_3\mathrm{e}^{-\lambda\hat{\tau}_{0,0}}}, \tag{81}$$

$$I_{1,0}^{\mathrm{C}} = 2\frac{O_3\left(\lambda\hat{h}_{0,1} + b_1\mathrm{e}^{-\lambda\hat{\tau}_{0,0}}\right) - \left[(1-k)(1+\hat{E}_{0,0})\hat{h}_{0,1} + b_3\right]b_2}{-O_1O_2\mathrm{e}^{-\lambda\hat{\tau}_{0,0}} - \lambda O_1(1+\lambda\hat{\tau}_{0,0}) + M_{\mathrm{C}}O_3\mathrm{e}^{-\lambda\hat{\tau}_{0,0}}}, \tag{82}$$

$$\hat{\tau}_{1,0} = 2\lambda\bar{G}I_{0,0}^2\mathrm{e}^{-\lambda\hat{\tau}_{0,0}}Z_3(\hat{\tau}_{0,0},\lambda) + \frac{2}{\lambda}\bar{G}M_{\mathrm{C}}I_{0,0}I_{0,0}^{\mathrm{C}}\mathrm{e}^{-\lambda\hat{\tau}_{0,0}}Z_4(\hat{\tau}_{0,0},\lambda), \tag{83}$$

$$I_{1,1} = \frac{\lambda(2+\lambda\hat{\tau}_{0,0})(O_1b_1 - M_{\mathrm{C}}b_3)}{-O_1O_2\mathrm{e}^{-\lambda\hat{\tau}_{0,0}} - \lambda(2+\lambda\hat{\tau}_{0,0})O_1 + M_{\mathrm{C}}O_4\mathrm{e}^{-\lambda\hat{\tau}_{0,0}}}, \tag{84}$$

$$I_{1,1}^{\mathrm{C}} = \frac{(O_2b_3 - O_4b_1)\mathrm{e}^{-\lambda\hat{\tau}_{0,0}} + \lambda(2+\lambda\hat{\tau}_{0,0})b_3}{-O_1O_2\mathrm{e}^{-\lambda\hat{\tau}_{0,0}} - \lambda(2+\lambda\hat{\tau}_{0,0})O_1 + M_{\mathrm{C}}O_4\mathrm{e}^{-\lambda\hat{\tau}_{0,0}}}, \tag{85}$$

$$\hat{h}_{0,1} = \lambda\bar{G}I_{0,0}^2\mathrm{e}^{-\lambda\hat{\tau}_{0,0}}Z_1(\hat{\tau}_{0,0},\lambda) + \frac{1}{\lambda}\bar{G}M_{\mathrm{C}}I_{0,0}I_{0,0}^{\mathrm{C}}\mathrm{e}^{-\lambda\hat{\tau}_{0,0}}Z_2(\hat{\tau}_{0,0},\lambda), \tag{86}$$

where

$$Z_1(\hat{\tau}_{0,0},\lambda)=\frac{O_1\hat{R}_0(\hat{\tau}_{0,0})}{-O_1O_2\,\mathrm{e}^{-\lambda\hat{\tau}_{0,0}}-\lambda(2+\lambda\hat{\tau}_{0,0})O_1+M_{\mathrm{C}}O_4\,\mathrm{e}^{-\lambda\hat{\tau}_{0,0}}},$$

$$Z_2(\hat{\tau}_{0,0},\lambda)=\frac{[O_1-(1-k)\hat{\tau}_{0,0}]\hat{R}_1(\hat{\tau}_{0,0})}{-O_1O_2\,\mathrm{e}^{-\lambda\hat{\tau}_{0,0}}-\lambda(2+\lambda\hat{\tau}_{0,0})O_1+M_{\mathrm{C}}O_4\,\mathrm{e}^{-\lambda\hat{\tau}_{0,0}}},$$

$$Z_3[\hat{\tau}_{0,0},\lambda]=\frac{-\left(O_2\,\mathrm{e}^{-\lambda\hat{\tau}_{0,0}}+\lambda\,\mathrm{e}^{-\lambda\hat{\tau}_{0,0}}+\lambda O_1\right)Z_1(\hat{\tau}_{0,0},\lambda)\ -O_1\hat{R}_0(\hat{\tau}_{0,0})}{-O_1O_2\,\mathrm{e}^{-\lambda\hat{\tau}_{0,0}}-\lambda O_1(1+\lambda\hat{\tau}_{0,0})+M_{\mathrm{C}}O_3\,\mathrm{e}^{-\lambda\hat{\tau}_{0,0}}},$$

$$Z_4(\hat{\tau}_{0,0},\lambda)=\frac{-\left[(O_2+\lambda)\,\mathrm{e}^{-\lambda\hat{\tau}_{0,0}}+\lambda O_1\right]Z_2(\hat{\tau}_{0,0},\lambda)\ +[(1-k)\hat{\tau}_{0,0}-O_1]\hat{R}_1(\hat{\tau}_{0,0})}{-O_1O_2\,\mathrm{e}^{-\lambda\hat{\tau}_{0,0}}-\lambda O_1(1+\lambda\hat{\tau}_{0,0})+M_{\mathrm{C}}O_3\,\mathrm{e}^{-\lambda\hat{\tau}_{0,0}}},$$

in which O_1, O_2, O_3, O_4, b_1, b_2, b_3 are seven abbreviations

$$\begin{aligned}
O_1&=(1-k)\hat{\tau}_{0,0}-\mathrm{e}^{-\hat{\tau}_{0,0}},\\
O_2&=-\lambda-(1-k)M_{\mathrm{C}}[1+\hat{E}_{0,0}(\hat{\tau}_{0,0})],\\
O_3&=(1-k)(1+k\hat{\tau}_{0,0})(1+\hat{E}_{0,0}),\\
O_4&=(1-k)(2+k\hat{\tau}_{0,0})(1+\hat{E}_{0,0}),\\
b_1&=\lambda\bar{G}I_{0,0}^2\hat{R}_0(\hat{\tau}_{0,0})+\frac{1}{\lambda}\bar{G}M_{\mathrm{C}}I_{0,0}I_{0,0}^{\mathrm{C}}\hat{R}_1(\hat{\tau}_{0,0}),\\
b_2&=\lambda(1+\lambda\hat{\tau}_{0,0})+O_2\,\mathrm{e}^{-\lambda\hat{\tau}_{0,0}},\\
b_3&=\frac{1}{\lambda}(1-k)\bar{G}I_{0,0}I_{0,0}^{\mathrm{C}}\hat{\tau}_{0,0}\hat{R}_1(\hat{\tau}_{0,0}).
\end{aligned}$$

Thus we obtain the inner solution for the temperature and concentration fields

$$\begin{aligned}
T_{\mathrm{L}}&=T_\infty+\lambda\hat{\tau}_{0,0}\,\mathrm{e}^{\lambda\hat{\tau}_{0,0}}E_1(\lambda\hat{\tau})\\
&\quad+\varepsilon^4[(I_{1,0}E_1(\lambda\hat{\tau})-2\lambda\bar{G}I_{0,0}^2\hat{R}_0(\hat{\tau}))\\
&\quad+\bar{\sigma}(I_{1,1}E_1(\lambda\hat{\tau})+\lambda\bar{G}I_{0,0}^2\hat{R}_0(\hat{\tau}))]+\cdots, \qquad (87)\\
C_{\mathrm{L}}&=1+\frac{\tilde{\tau}_{0,0}(1-k)\,\mathrm{e}^{\tilde{\tau}_{0,0}}}{1-(1-k)\tilde{\tau}_{0,0}E_1(\tilde{\tau}_{0,0})\,\mathrm{e}^{\tilde{\tau}_{0,0}}}E_1(\tilde{\tau})\\
&\quad+\varepsilon^4[(I_{1,0}^{\mathrm{C}}E_1(\hat{\tau})-\frac{2}{\lambda}\bar{G}I_{0,0}I_{0,0}^{\mathrm{C}}\hat{R}_1(\hat{\tau}))\\
&\quad+\bar{\sigma}(I_{1,1}^{\mathrm{C}}E_1(\hat{\tau})+\frac{1}{\lambda}\bar{G}I_{0,0}I_{0,0}^{\mathrm{C}}\hat{R}_1(\hat{\tau}))]+\cdots. \qquad (88)
\end{aligned}$$

And the interface shape function

$$\hat{\tau}=\hat{\tau}_{\mathrm{S}}=\hat{\tau}_{0,0}+\varepsilon^4\left(\hat{\tau}_{1,0}+\hat{h}_{0,1}\bar{\sigma}\right)+\cdots, \qquad (89)$$

$$\eta_{\mathrm{S}}^2=1+\varepsilon^4\frac{\hat{h}_{0,1}}{\hat{\tau}_{0,0}}\bar{\sigma}+\cdots. \qquad (90)$$

It is easily proved that Eqs. (87) and (88) satisfy the far field conditions, i.e., as $\tau\to\infty$ or $\eta\to\infty$,

$$T_{\mathrm{L}}\to T_\infty,\quad C_{\mathrm{L}}\to 1. \qquad (91)$$

Consequently, the outer solution for the temperature and concentration fields in the outer region are not necessary.

The normalization parameter becomes

$$\begin{aligned}
\eta_0^2&=2\hat{\tau}_{0,0}+4\varepsilon^4\bar{G}\,\mathrm{e}^{-\lambda\hat{\tau}_{0,0}}\left[\lambda I_{0,0}^2Z_3(\hat{\tau}_{0,0},\lambda)\right.\\
&\quad\left.+\frac{1}{\lambda}M_{\mathrm{C}}I_{0,0}I_{0,0}^{\mathrm{C}}Z_4(\hat{\tau}_{0,0},\lambda)\right]+\cdots\\
&=2\hat{\tau}_{0,0}+\frac{8}{|T_\infty|}\frac{Gr}{S_{\mathrm{C}}}\,\mathrm{e}^{-\lambda\hat{\tau}_{0,0}}\left[\lambda I_{0,0}^2Z_3(\hat{\tau}_{0,0},\lambda)\right.\\
&\quad\left.+\frac{1}{\lambda}M_{\mathrm{C}}I_{0,0}I_{0,0}^{\mathrm{C}}Z_4(\hat{\tau}_{0,0},\lambda)\right]+\cdots. \qquad (92)
\end{aligned}$$

The twice mean curvature of the tip is

$$K(0)=\frac{2}{\eta_0^2}\left(1-\frac{\eta_0^2}{S_{\mathrm{C}}}\frac{\mathrm{d}}{\mathrm{d}\bar{\sigma}}\eta_{\mathrm{S}}(0)\right).$$

The Peclet number Pe, which is defined as $Pe=\lambda\ell_t/\ell_{\mathrm{D}}$, and ℓ_t is the tip radius, becomes

$$\begin{aligned}
Pe&=\lambda\frac{2}{K(0)}\\
&=Pe_0\left\{1+\frac{Gr}{S_{\mathrm{C}}^2}\frac{2\,\mathrm{e}^{-\lambda\hat{\tau}_{0,0}}}{|T_\infty|}\left[\lambda I_{0,0}^2Z_1(\hat{\tau}_{0,0},\lambda)\right.\right.\\
&\quad\left.+\frac{1}{\lambda}M_{\mathrm{C}}I_{0,0}I_{0,0}^{\mathrm{C}}Z_2(\hat{\tau}_{0,0},\lambda)\right]\\
&\quad+\frac{Gr}{S_{\mathrm{C}}}\frac{4\,\mathrm{e}^{-\lambda\hat{\tau}_{0,0}}}{\hat{\tau}_{0,0}|T_\infty|}\left[\lambda I_{0,0}^2Z_3(\hat{\tau}_{0,0},\lambda)\right.\\
&\quad\left.\left.+\frac{1}{\lambda}M_{\mathrm{C}}I_{0,0}I_{0,0}^{\mathrm{C}}Z_4(\hat{\tau}_{0,0},\lambda)\right]\right\}, \qquad (93)
\end{aligned}$$

where Pe_0 represents the Peclet number that is not affected by the buoyant flow

$$Pe_0=\lambda\eta_{0,0}^2=2\lambda\hat{\tau}_{0,0}. \qquad (94)$$

The interface shape function is expressed as

$$\eta_{\mathrm{S}}=\eta_{\mathrm{S}}(\xi,\varepsilon)\approx\sqrt{1+\frac{2\,\mathrm{e}^{-\lambda\hat{\tau}_{0,0}}}{|T_\infty|}\frac{Gr}{S_{\mathrm{C}}^2}\left[\lambda I_{0,0}^2Z_1(\hat{\tau}_{0,0},\lambda)+\frac{1}{\lambda}M_{\mathrm{C}}I_{0,0}I_{0,0}^{\mathrm{C}}Z_2(\hat{\tau}_{0,0},\lambda)\right]\xi^2}. \qquad (95)$$

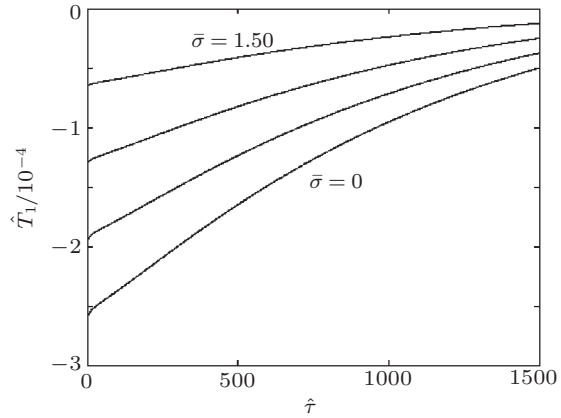


Fig. 5. The variations of solution $\hat{T}_1$ with variable $\hat{\tau}$ in the binary melt for the cases: $\bar{\sigma} = 0$, 0.50, 1.00, 1.50 from bottom to top in the undercooled binary melt with $\hat{\tau}_{0,0} = 0.2$, $k = 0.3$, $\lambda = 0.001$, and $M_C = 0.30$.

In Figs. 5–8, we respectively show the variations of the temperature $\hat{T}_1$ and concentration $\hat{C}_1$ versus the variable $\hat{\tau}$ for the cases: $\hat{\tau}_{0,0} = 0.2$ and $\hat{\tau}_{0,0} = 2.0$ in which $k = 0.30$, $\lambda = 0.001$. In Figs. 9–10, we respectively show the function $\hat{h}_{0,1}$ and $\hat{\tau}_{1,0}$ versus the variable $\hat{\tau}_{0,0}$ for the cases: $M_C = 0.1, 0.5, 1.0, 1.5, 2.0$, and $k = 0.30$, $\lambda = 0.001$. It can be seen from Fig. 9(a) that $\hat{\tau}_{0,0}$ is less than some critical values, the function $\hat{h}_{0,1}$ is always negative and the smaller morphology number corresponds to the lower value of the function $\hat{h}_{0,1}$, whereas from Fig. 9(b) that when $\hat{\tau}_{0,0}$ increases larger than the critical value, the function $\hat{h}_{0,1}$ is always positive and the smaller morphology number corresponds to the higher value of the function $\hat{h}_{0,1}$. As $\hat{\tau}_{0,0}$ further increases, the function $\hat{h}_{0,1}$ diminishes eventually. When $\hat{\tau}_{0,0}$ is less than some critical values (as seen in Fig. 10(a)), the function $\hat{\tau}_{1,0}$ is always positive and the smaller morphology number corresponds to the higher value of the function $\hat{h}_{0,1}$, whereas when $\hat{\tau}_{0,0}$ increases larger than the critical value (as seen in Fig. 10(b)), the function $\hat{\tau}_{1,0}$ is always negative and the smaller morphology number corresponds to the lower value of the function $\hat{\tau}_{1,0}$. As $\hat{\tau}_{0,0}$ further increases, the function $\hat{\tau}_{1,0}$ diminishes eventually. It implies that the morphology number plays an active role in the change of the interface and leads to the buoyancy effect that is different from the situation for the pure melt. The smaller the morphology number is, the more significant change the interface shape of the dendrite has. Thus, we can see from Eq. (91) that the normalization parameter is mainly changed by the function $\hat{\tau}_{1,0}$ and the change of the Peclet number comes from the contributions of the function $\hat{\tau}_{1,0}$ and the function $\hat{h}_{0,1}$, and from Eq. (92) that the function $\hat{\tau}_{1,0}$, together with the function $\hat{h}_{0,1}$, contributes the change of the Peclet number Pe. The interface function Eq. (94) shows the interface function is mainly changed by the function $\hat{h}_{0,1}$. Figures 11 and 12 illustrate that for the Grashof number $Gr > 0$, when the Peclet number Pe_0 (or equivalently, $\hat{\tau}_{0,0}$) is less than some critical value, the interface shape of the dendrite becomes thinner as the Grashof number increases, whereas when Pe_0 (or equivalently, $\hat{\tau}_{0,0}$) increases larger than the critical value, the interface shape becomes fatter as the Grashof number increases. When Pe_0 further increases (as we see from Fig. 9), the effect of buoyancy on the interface diminishes eventually.

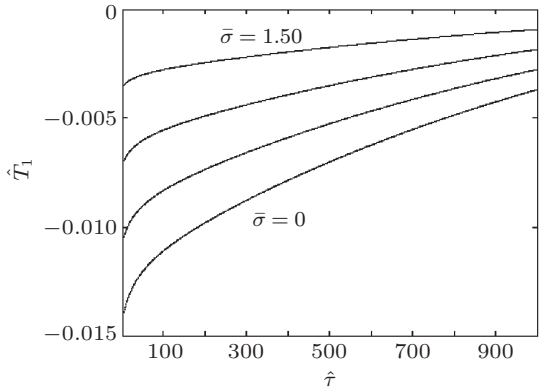


Fig. 6. The variations of solution $\hat{T}_1$ with variable $\hat{\tau}$ for the cases: $\bar{\sigma} = 0$, 0.50, 1.00, 1.50 from bottom to top in the undercooled binary melt with $\hat{\tau}_{0,0} = 2$, $k = 0.3$, $\lambda = 0.001$, and $M_C = 0.30$.

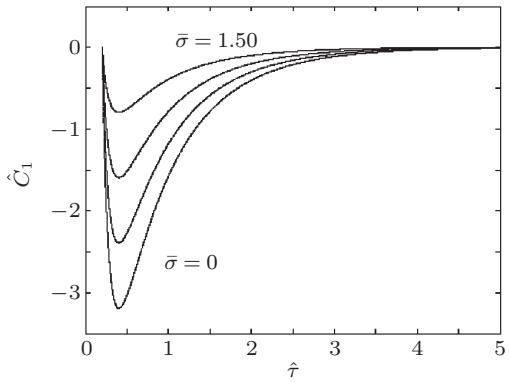


Fig. 7. The variations of solution $\hat{C}_1$ with variable $\hat{\tau}$ for the cases: $\bar{\sigma} = 0$, 0.50, 1.00, 1.50 from bottom to top in the undercooled binary melt with $\hat{\tau}_{0,0} = 0.20$, $k = 0.3$, $\lambda = 0.01$, and $M_C = 0.30$.

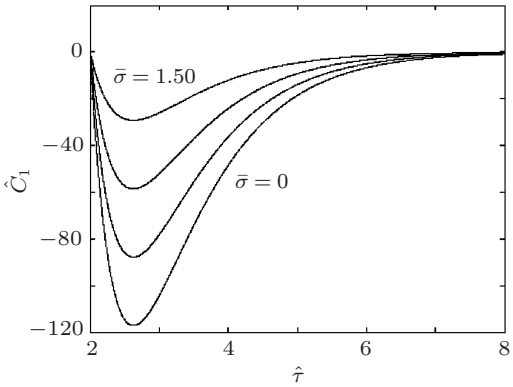


Fig. 8. The variations of solution $\hat{C}_1$ with variable $\hat{\tau}$ for the cases: $\bar{\sigma} = 0$, 0.50, 1.00, 1.50 from bottom to top in the undercooled binary melt with $\hat{\tau}_{0,0} = 2.0$, $k = 0.3$, $\lambda = 0.001$, and $M_C = 0.30$.

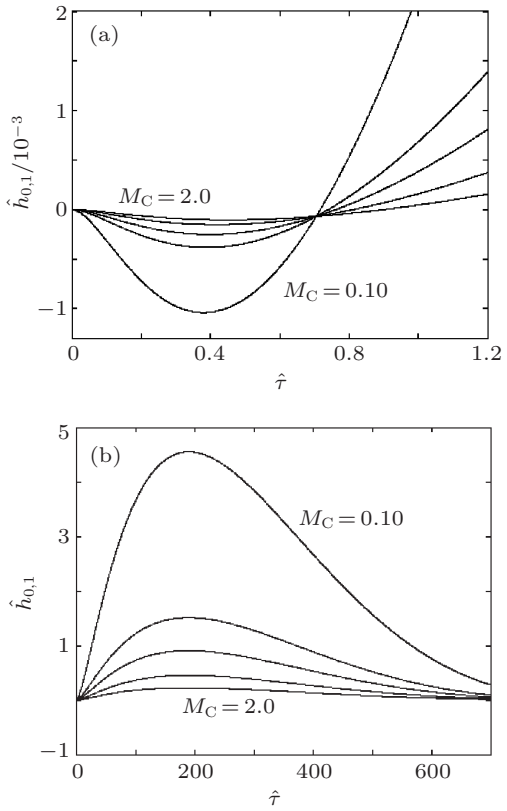


Fig. 9. The variations of function $\hat{h}_{0,1}$ versus variable $\hat{\tau}_{0,0}$ for the cases: $M_C = 0.1$, 0.5, 1.0, 1.5, 2.0 (a) from bottom to top; (b) from top to bottom in the undercooled binary melt with $k = 0.3$, $\lambda = 0.001$.

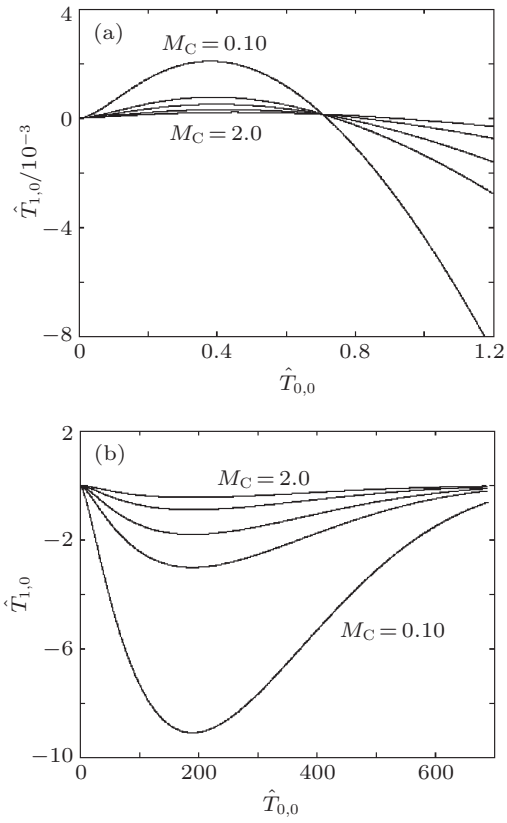


Fig. 10. The variations of function $\hat{\tau}_{1,0}$ versus variable $\hat{\tau}_{0,0}$ for the cases: $M_C = 0.1$, 0.5, 1.0, 1.5, 2.0 (a) from top to bottom; (b) from bottom to top in the undercooled binary melt with $k = 0.3$, $\lambda = 0.001$.

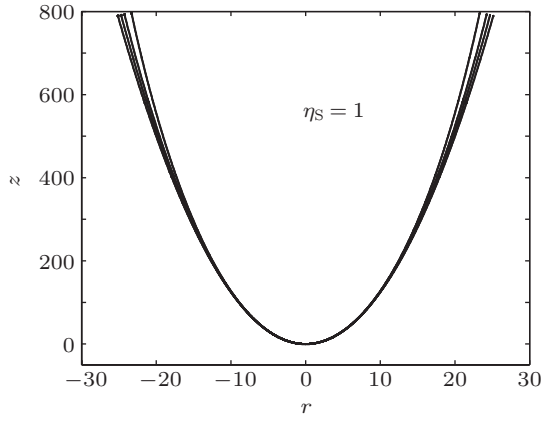


Fig. 11. The interface shapes for the cases: $Gr = 0$, 0.50, 1.0, 2.0 from outside to inside in the binary melt with $Pe_0 = 0.0004$ (or $\hat{\tau}_{0,0} = 0.2$), $S_C = 20$, $k = 0.3$, $\lambda = 0.001$, and $M_C = 0.20$.

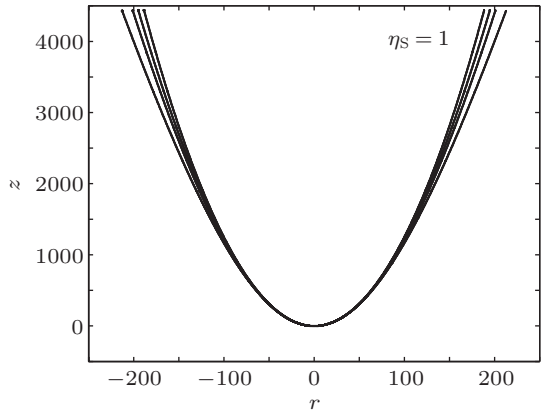


Fig. 12. The interface shapes for the cases: $Gr = 0$, 0.50, 1.0, 2.0 from inside to outside in the binary melt with $Pe_0 = 0.004$ (or $\hat{\tau}_{0,0} = 2.0$), $S_C = 20$, $k = 0.3$, $\lambda = 0.001$, and $M_C = 0.20$.

4. Conclusion

We have studied the effect of buoyancy-driven convection on the steady state dendritic growth with zero surface tension and zero kinetic undercooling in an undercooled binary alloy. For the case of the moderate modified Grashof number, by using the matched asymptotic expansion method, we obtain the uniformly valid asymptotic solution in the entire region of space. The analytical result shows that the temperature field plays an active role and the perturbed flow field and concentration field are passive. The interactions between the temperature field and flow field and between the concentration field and flow field are only through their inner solutions. The zeroth-order inner solution of the temperature field determines the zeroth-order inner solution of induced flow field, then the zeroth-order inner solution of the induced flow field affects the temperature field, concentration field, and interface shape, resulting in the first-order correction of the temperature and concentration fields and the interface shape.

Due to the buoyancy-induced convection in the undercooled binary alloy, the interface shape of needle-like crystal is changed. The interface shape depends on four parameters:

undercooling T_∞, Peclet number Pe_0, Grashof number Gr, and morphology number M_C. When the Peclet number Pe_0 is less than some critical value, the interface shape of the dendrite becomes thinner as the Grashof number Gr becomes larger, whereas when Pe_0 is larger than the critical value, the interface shape becomes fatter as the Grashof number Gr increases. The smaller the morphology number is, the more significant change the interface shape of the dendrite has. In the undercooled binary alloy, the morphology number plays an active role in the change of the interface and leads to the significant buoyancy effect that is different from the situation for the pure melt. Due to the buoyancy-induced convection, the normalization parameter and the Peclet number are changed. As the Peclet number further increases, the effect of buoyancy on the interface diminishes eventually.

Acknowledgments

The authors wish to thank Prof. Xu Jian-Jun (McGill University, Canada; University of Science and Technology Beijing, Beijing) for his instructive help.

Appendix A

The inner solution equations and interface conditions for the temperature field and concentration field

The inner solution equations

$$\begin{aligned}&\varepsilon\bar{\sigma}\frac{\partial^2\hat{T}_{\rm L}}{\partial\bar{\sigma}^2}+\varepsilon\frac{\partial\hat{T}_{\rm L}}{\partial\bar{\sigma}}+\hat{\tau}\frac{\partial^2\hat{T}_{\rm L}}{\partial\hat{\tau}^2}+\frac{\partial\hat{T}_{\rm L}}{\partial\hat{\tau}}\\&=\lambda\left(\bar{\sigma}\frac{\partial\hat{T}_{\rm L}}{\partial\bar{\sigma}}-\hat{\tau}\frac{\partial\hat{T}_{\rm L}}{\partial\hat{\tau}}\right)+\frac{\lambda\varepsilon}{2}\frac{\partial(\hat{T}_{\rm L},\hat{\psi})}{\partial(\bar{\sigma},\hat{\tau})},\end{aligned}\tag{A1}$$

$$\begin{aligned}&\varepsilon\bar{\sigma}\frac{\partial^2\hat{C}}{\partial\bar{\sigma}^2}+\varepsilon\frac{\partial\hat{C}}{\partial\bar{\sigma}}+\hat{\tau}\frac{\partial^2\hat{C}}{\partial\hat{\tau}^2}+\frac{\partial\hat{C}}{\partial\hat{\tau}}\\&=\left(\bar{\sigma}\frac{\partial\hat{C}}{\partial\bar{\sigma}}-\hat{\tau}\frac{\partial\hat{C}}{\partial\hat{\tau}}\right)+\frac{\varepsilon}{2}\frac{\partial(\hat{C},\hat{\psi})}{\partial(\bar{\sigma},\hat{\tau})}.\end{aligned}\tag{A2}$$

The interface conditions: at the interface $\hat{\tau}=\hat{\tau}_{0,0}$

$$\begin{aligned}&\varepsilon(T_\infty+M_{\rm C})+\hat{T}_{\rm L}+\frac{\partial\hat{T}_{\rm L}}{\partial\hat{\tau}}(\tilde{\tau}_0+\hat{h}_{\rm S})+\cdots\\&+M_{\rm C}\left[\hat{C}_{\rm L}+\frac{\partial\hat{C}_{\rm L}}{\partial\hat{\tau}}(\tilde{\tau}_0+\hat{h}_{\rm S})+\cdots\right]=0,\end{aligned}\tag{A3}$$

$$\begin{aligned}&\frac{1}{\lambda}(\hat{\tau}_{0,0}+\tilde{\tau}_0+\hat{h}_{\rm S})\left[\frac{\partial\hat{T}_{\rm L}}{\partial\hat{\tau}}+\frac{\partial^2\hat{T}_{\rm L}}{\partial\hat{\tau}^2}(\tilde{\tau}_0+\hat{h}_{\rm S})+\cdots\right]\\&-\varepsilon\bar{\sigma}(\hat{h}_{\rm S})'\frac{1}{\lambda}\left[\frac{\partial\hat{T}_{\rm L}}{\partial\bar{\sigma}}+\frac{\partial^2\hat{T}_{\rm L}}{\partial\bar{\sigma}\partial\hat{\tau}}(\tilde{\tau}_0+\hat{h}_{\rm S})+\cdots\right]\\&+\varepsilon[\hat{\tau}_{0,0}+\tilde{\tau}_0+\hat{h}_{\rm S}+\bar{\sigma}(\hat{h}_{\rm S})']=0,\end{aligned}\tag{A4}$$

$$\begin{aligned}&(1-k)[\hat{\tau}_{0,0}+\tilde{\tau}_0+\hat{h}_{\rm S}+\bar{\sigma}(\hat{h}_{\rm S})']\left[\hat{C}_{\rm L}+\frac{\partial\hat{C}_{\rm L}}{\partial\hat{\tau}}(\tilde{\tau}_0+\hat{h}_{\rm S})+\cdots\right]\\&+\varepsilon(1-k)[\hat{\tau}_{0,0}+\tilde{\tau}_0+\hat{h}_{\rm S}+\bar{\sigma}(\hat{h}_{\rm S})']+\lambda_0(\hat{\tau}_{0,0}+\tilde{\tau}_0\\&+\hat{h}_{\rm S})\left[\frac{\partial\hat{C}_{\rm L}}{\partial\hat{\tau}}+\frac{\partial^2\hat{C}_{\rm L}}{\partial\hat{\tau}^2}(\tilde{\tau}_0+\hat{h}_{\rm S})+\cdots\right]\\&+\varepsilon\bar{\sigma}(\hat{h}_{\rm S})'\left[\frac{\partial\hat{C}_{\rm L}}{\partial\bar{\sigma}}+\frac{\partial^2\hat{C}_{\rm L}}{\partial\bar{\sigma}\partial\hat{\tau}}(\tilde{\tau}_0+\hat{h}_{\rm S})+\cdots\right]=0.\end{aligned}\tag{A5}$$

Equations (A1) and (A2) have the solution of the Laguerre series expansions

$$\begin{aligned}\hat{T}_{\rm L}&=\sum_{n=0}^{\infty}\hat{D}_n(\hat{\tau},\varepsilon_2)L_n^{(1)}(\bar{\sigma}),\\\hat{C}&=\sum_{n=0}^{\infty}\hat{E}_n(\hat{\tau},\varepsilon_2)L_n^{(1)}(\bar{\sigma}),\end{aligned}\tag{A6}$$

from Eqs. (A3)–(A5), we have

$$\begin{aligned}&\hat{\tau}\frac{{\rm d}^2\hat{D}_n}{{\rm d}\hat{\tau}^2}+(1+\lambda\hat{\tau})\frac{{\rm d}\hat{D}_n}{{\rm d}\hat{\tau}}-\lambda n\hat{D}_n\\&=-\lambda(n+2)\hat{D}_{n+1}+\varepsilon(n+1)\hat{D}_{n+1}\\&\quad-\varepsilon\sum_{m=n+2}^{\infty}\hat{D}_n+\frac{\lambda\varepsilon}{2}N(\hat{D}_n,\hat{B}_n),\end{aligned}\tag{A7}$$

$$\begin{aligned}&\hat{\tau}\frac{{\rm d}^2\hat{E}_n}{{\rm d}\hat{\tau}^2}+(1+\hat{\tau})\frac{{\rm d}\hat{E}_n}{{\rm d}\hat{\tau}}-n\hat{E}_n\\&=-(n+2)\hat{E}_{n+1}+\varepsilon(n+1)\hat{E}_{n+1}\\&\quad-\varepsilon\sum_{m=n+2}^{\infty}\hat{E}_n+\frac{\varepsilon}{2}N(\hat{E}_n,\hat{B}_n),\end{aligned}\tag{A8}$$

where $N(\hat{D}_n,\hat{B}_n)$ and $N(\hat{E}_n,\hat{B}_n)$ are the coefficients of the Laguerre function in the asymptotic expansion of Jacobian determinants $\partial(\hat{T}_{\rm L},\hat{\psi})/\partial(\bar{\sigma},\hat{\tau})$ and $\partial(\hat{C}_{\rm L},\hat{\psi})/\partial(\bar{\sigma},\hat{\tau})$.

References

[1] Huang S C and Glicksman M E 1981 *Acta Metal.* **29** 701
[2] Lee Y W and Gill W N 1992 *Chem. Eng. Comm.* **116** 193
[3] Rubinstein E R and Glicksman M E 1991 *J. Crystal Growth* **112** 84
[4] Shi Y F, Xu Q Y and Liu B C 2011 *Acta Phys. Sin.* **60** 126101 (in Chinese)
[5] Liu R P, Zhao J H, Zhang X Y, He R W, Xu Y F and Wang W K 1998 *Acta Phys. Sin.* **47** 1571 (in Chinese)
[6] Li J J, Wang J C and Yang G C 2007 *J. Cryst. Growth* **309** 65
[7] Baumgartl J, Budweiser W, Müller G and Neumann G 1989 *J. Crystal Growth* **97** 9
[8] Lee Y W, Smith R N, Glicksman M E and Koss M B 1996 *Annual Rev. of Heat Transfer* **7** 59
[9] Cai L X, Jin W Q, Yoda S, Pan Z L, Liang X A and Liu Z H 2001 *J. Crystal Growth* **231** 230
[10] Basil N A, Mark S P and William K W 2003 *J. Crystal Growth* **250** 565
[11] Ananth R and Gill W N 1988 *J. Crystal Growth* **91** 587
[12] Schrage D S 1999 *J. Crystal Growth* **205** 410
[13] Huo C R, Zhu Z H, Ge P W and Chen D 2001 *Acta Phys. Sin.* **50** 377 (in Chinese)
[14] Zhu Z H, Ge P W, Huo C R and Xu Z Y 1998 *Acta Phys. Sin. (Oversees edn.)* **7** 801
[15] Huo C R, Xu Z Y, Huang W D, Ge P W and Zhu Z H 1996 *J. Crystal Growth* **158** 359
[16] Huo C R, Zhu Z H, Ge P W and Chen D 2001 *Acta Phys. Sin.* **50** 377 (in Chinese)
[17] Ge P W, Nishinaga T, Li C R, Huo C R, Nakamura T, Huang W D Voloshin A E and Lomov A A 2001 *Sci. China A* **44** 762
[18] Liu R P, Zhao J H, Zhang X Y, He D W, Xu Y F and Wang W K 1998 *Acta Phys. Sin.* **47** 1571 (in Chinese)
[19] Canright D and Davis S H 1991 *J. Crystal Growth* **114** 153
[20] Xu J J 2004 *Dynamical Theory of Dendritic Growth in Convective Flow* (Berlin: Springer)
[21] Xu J J 2006 *J. Crystal Growth* **292** 523
[22] Chen M W, Wang X F, Wang Z D and Xie J X 2008 *J. Cryst. Growth* **310** 655
[23] Ivantsov G P 1947 *Dokl. Akad. Nauk, SSSR* **58** 567